

AEM ANALYSIS OF GRID-STEEL PLATE RETROFITTING METHOD FOR MASONRY PIERS OF RAILWAY BRIDGES

Ngoc T. PHAN*1, Akira HOSODA*2, Hamed SALEM*3 and Sakiko TAKAHASHI*4

ABSTRACT

The effects of grid-steel plates to enhance the seismic performance of masonry pier of railway bridges were experimentally studied and numerically investigated by Applied Element Method (AEM). By improving the details of grid-steel plate retrofitting method, sliding of blocks could be eliminated and rocking behavior of a retrofitted column was observed. AEM simulation with appropriate modeling of boundary surfaces between concrete blocks and PVC sheet showed acceptable simulation results.

Keywords: Applied Element Method (AEM), grid-steel plate retrofitting method, masonry piers

1. INTRODUCTION

In the metropolitan area in Japan, there are some old railway bridges in service that are made of unreinforced masonry bricks or stones. Past and recent researches have shown that unreinforced masonry piers of railway bridges have poorly performed under seismic actions. Horizontal sliding and large residual displacement of bricklayers at the mortar joints are major causes of catastrophic failure (Fig.1) [1].

Partial steel plate retrofitting method was proposed by Tadokoro, et.al [2] where two steel plates were attached to cover the side surfaces of a masonry pier and embedded into the footing by steel bar anchors. The retrofitted brick pier then performed like an RC column [2].

In this research, a new method named grid-steel plate retrofitting method, different from the method by Tadokoro, et al, is developed. This method is aimed to prevent sliding at the joints and spalling of blocks, and it is not aimed to increase the capacity of piers by anchoring to the footing. As the first step of this development, two separated concrete blocks were retrofitted by the newly developed grid-steel plate retrofitting method and static cyclic loading was conducted (Fig.2). Numerical simulations by Applied Element Method were conducted and verified by the experimental results.

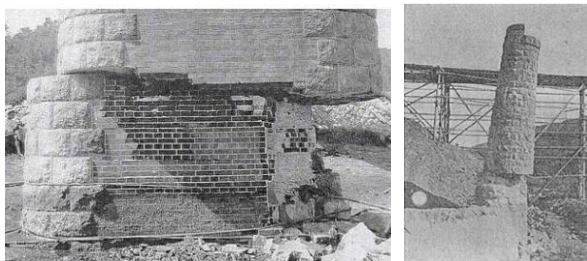


Fig.1 Damages of Minatogawa and Chitosegawa bridge in Great Kanto earthquake (1923)

2. CONCEPT OF THE GRID-STEEL PLATE RETROFITTING METHOD

Due to the very limited space around many existing masonry railway bridge piers and abutments, it is difficult to apply jacketing retrofitting methods in some cases. The concept of the retrofitting method in this research is to prevent horizontal sliding at the joints minimizing residual displacement which lead to difficulty in restoration after earthquakes (Fig.2). Spalling of blocks should also be mitigated by this method. The rocking behavior instead of sliding of bricklayers in the retrofitted pier is expected to perform under seismic actions (Fig.3). At the final step, to give sufficient seismic performance for the whole bridge system, the brackets will be attached to the upper girders to prevent the piers from falling or overturning.

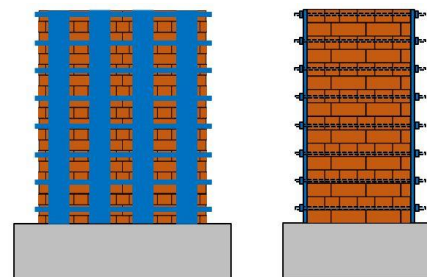


Fig.2 The Grid-steel plate retrofitting method

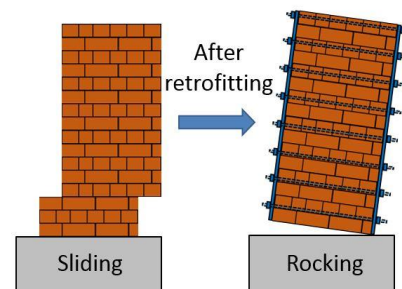


Fig.3 The performance of retrofitted piers

*1 Graduate student, Graduate School of Urban Innovation, Yokohama National University, JCI Member
 *2 Professor, Institute of Urban Innovation, Yokohama National University, Dr.E., JCI Member
 *3 Professor, Structural Engineering Department, Cairo University, Egypt
 *4 Assistant Manager, Structural Engineering Center, East Japan railway company, JCI member

3. EXPERIMENTAL PROGRAM

In this study, separated two concrete blocks with small friction between them are used to check the effectiveness of grid-steel plate retrofitting methods. In the future, retrofitted masonry specimens made of bricks will be conducted.

3.1 Detail of specimen

The experimental program consists of 3 specimens named Case 1, Case 2, Case 3. The grid-steel plate method is improved learning from the experimental results of each case, resulting in the alteration of the height (H) of the 600x600mm concrete blocks; and the alteration of width (b), length (l), thickness (t) and the arrangement of the steel plates, as shown in Table 1 and Table 2.

Table 1 Details of steel plates, steel anchors, sheath tubes and steel bars

Case	Steel plate SS400			Steel anchor			Sheath tube	Steel bar SR235
	t	b	l	t	b	l	ϕ	ϕ
	(mm)			(mm)			(mm)	(mm)
1	3	32	240	12	50	50	20	9
2	1.6	45	400	12	60	60	30	11
3	9	72	860	25	120	120	50	23

Table 2 Details of columns and PVC sheet

Case	Upper column			Lower column			PVC sheet
	H	b	h	H	b	h	t
	(mm)			(mm)			(mm)
1	1150	600	600	250	600	600	4
2	900	600	600	250	600	600	4
3	900	600	600	500	600	600	0.5

In the tests, two-separated concrete blocks were vertically jointed by pairs of steel plates, connected with penetrating round steel bars, as shown in Fig.4.

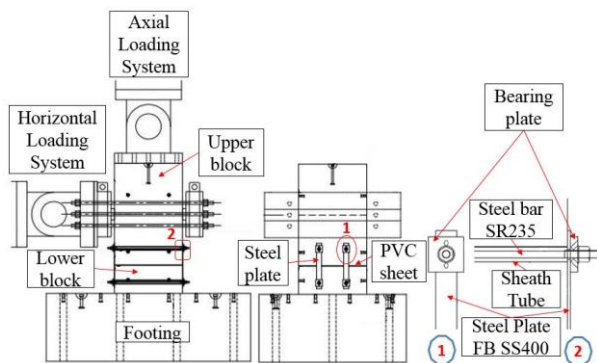


Fig.4 The main components of the specimen

A polyvinyl chloride (PVC) sheet was inserted between the joint of two concrete blocks to reduce the friction when horizontal load is applied to the specimen. The lower concrete block was placed on the hardened RC footing through a construction joint where the surface of the footing was made rough (Fig.4).

The interface material between steel plates and concrete columns was also investigated. In Case 1, epoxy resin was used for the interface. In Cases 2 and 3, spongy pads were inserted. The alternations of some components in the Case 2 and Case 3 were derived from the failure modes and undesired behavior of the specimens in the previous case.

3.2 Materials

The material properties of concrete and steel are shown in Table 3 and Table 4.

Table 3 Characteristics of concrete

Case	Concrete column		Concrete footing	
	average compressive strength (N/mm ²)	average tensile strength (N/mm ²)	average compressive strength (N/mm ²)	average tensile strength (N/mm ²)
1	19.4	2.98	29.9	3.76
2	42.1	4.42	43.6	4.41
3	46.0	3.4	42.9	4.51

Table 4 Characteristics of steel

Case	Steel plate SS400		Steel bar SR 235	
	yield stress (N/mm ²)	yield strain (μ)	yield stress (N/mm ²)	yield strain (μ)
1	379	1761	361	1723
2	329	1525	1104	7097
3	304	1460	1014	4886

3.3 Testing procedures

In the loading system, constant axial compressive load was kept and horizontal controlled displacement was applied.

In Case 1, only horizontal displacement was applied to the specimen. After cyclic horizontal displacements of ± 1 mm, ± 7 mm, ± 13 mm were given to the upper block, monotonic loading was applied until failure.

In Case 2, both axial compressive load and horizontal displacement were applied to the specimen. After 0.1N/mm² axial compressive stress was evenly distributed on the top of the upper block, cyclic horizontal displacements of ± 2 mm, ± 5 mm were applied, and after that monotonic loading was given to the upper block till failure.

In Case 3, the same axial compressive stress was applied as in Case 2 while cyclic horizontal displacements of ± 6 mm, ± 12 mm, ± 18 mm, ± 24 mm, ± 27 mm, ± 30 mm were applied, and after that monotonic loading was given to the upper block till failure (Fig.5).

3.4 Testing results

The load-displacement relationship in each case showed many sudden drops of horizontal load (Fig.5), which was acceptably explained due to friction between the PVC sheet and concrete blocks.

(1) Case 1

Fig.5 illustrates that in Case 1, there were some clear diagonal cracks generated in the region from the

steel bars to the top of the lower block. This diagonal cracking was caused due to punching shear by horizontal steel bars. The test was stopped when a steel bar in the lower concrete block was ruptured at the intersection with its connected steel plate, where the section of the steel bar was reduced due to its screw shape. For easy restoration after earthquakes, the damage of concrete blocks or the rupture of horizontal connecting steel bars should be avoided.

(2) Case 2

To prevent diagonal cracks observed in Case 1, the distance from the center of horizontal steel bars to the top of the lower concrete block was increased from 60mm to 150mm in Case 2. Moreover, in order to expect the rupture of the steel plates before the failure of the steel bars, the diameter of the steel bars was increased while less number of steel plates were used with thinner thickness. In addition, spongy pads of 60x60x6mm were used instead of epoxy resin to minimize undesirable high stress concentration due to contact of the steel plates to the concrete blocks in the initial stages of horizontal loading. There were some unexpected horizontal protrusions of the PVC sheet under cyclic horizontal loading causing early contact between the sheet and the steel plates. This unexpected early contact produced some tension in steel plates. Fig.5 describes that in Case 2, large spalling of cover concrete was observed at one side surface of the lower concrete block. The test was stopped when two steel plates were broken at the intersections with the steel bars, which was not a desirable failure pattern. No

crack was generated at the joint between concrete column and footing.

(3) Case 3

In Case 3, to expect rocking in the specimen, the thickness of steel plates was significantly increased. In addition, a PVC sheet with 0.5mm thickness which was thinner and softer than the one in Case 2 was used to minimize the effect of unexpected contact observed in Case 2. Moreover, the spongy pads of 120x120x12mm were set between the steel plates and the concrete blocks to prevent local failure of the plates. At the final stage of monotonic loading, the retrofitted column showed rocking at the base while the upper block showed a relative horizontal sliding of 16mm to the lower block.

4. THE APPLIED ELEMENT METHOD (AEM)

The AEM is a developed numerical analysis method following the concept of discrete cracking. In AEM, the structure is modeled as an assembly of small elements which are connected using their whole surfaces through a series of normal and shear springs. The stresses, strains, deformations, and failure of a certain part of the structure are entirely represented in each spring [3]. Once the springs connecting two adjacent elements are ruptured, these elements can be totally separated. This method, thus, can follow the structural behavior including crack initiation, propagation and load deformation from the initial loading stages till complete collapse with reliable

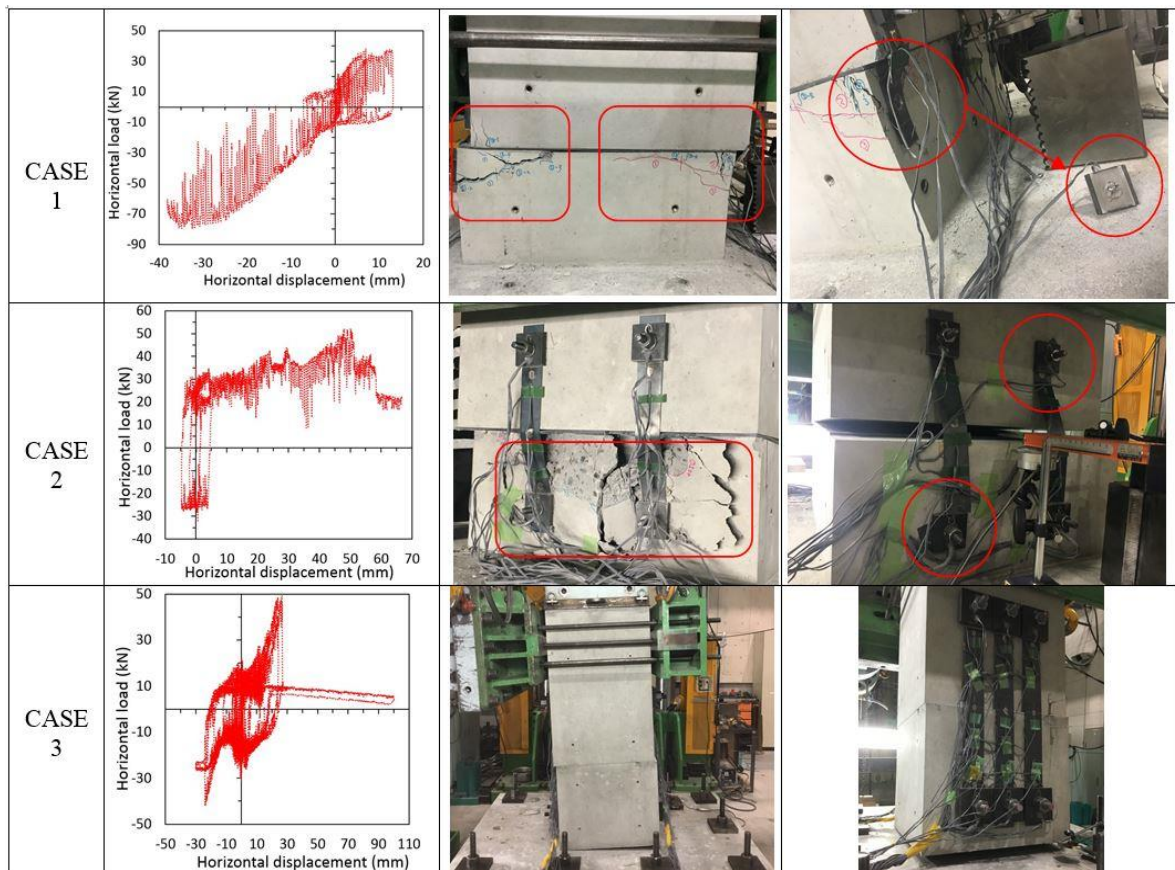


Fig.5 The performance of the specimens and experimental results

accuracy [4, 5]. In AEM, the nonlinear path-dependent constitutive models are adopted. The concrete material is followed the Maekawa compression model [6] (Fig.6a). For steel, the model represented by Ristic, et. al [7] is adopted (Fig.6b).

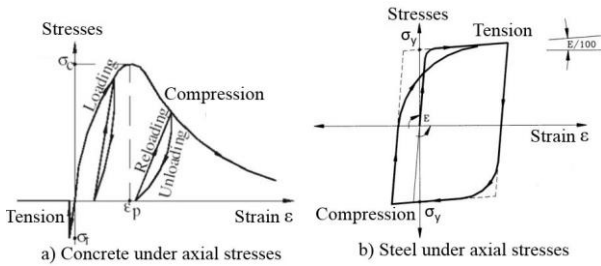


Fig.6 Concrete material model

In AEM the interface material is used to define the springs connecting two rigid bodies with different kinds of material [8]. In this research, bearing interface material was also utilized in which the material is initially cracked, and tensile stress cannot be carried. In the bearing interface material, the stress-strain relationship in compression is linear up to compression failure. The shear modulus is defined as G while μ is the coefficient of friction between the two surfaces [9]. For elastic interface material, where the stress-strain ratio is continuously constant, will behave linearly without plastic deformations or failure under normal and shear stresses [8].

5. VERIFICATION OF AEM SIMULATION

Here, load-displacement relationship, crack patterns in concrete specimens, failure patterns of the grid-steel plate systems, horizontal sliding at the joint of concrete blocks, etc. will be simulated by AEM.

For finding appropriate material input properties for the interface elements of AEM, calibration of important parameters was conducted in monotonic loading. The simulation results in monotonic loading until failure were compared to experimental load-displacement results until failure. After that, simulation results with calibrated parameters were verified by the experimental results in cyclic loading.

5.1 Case 1

The experimental results showed that loading capacity was governed by the strength of the steel plate retrofitting system and the sliding friction between the columns and the PVC sheet. In AEM, the interface material between the steel plates and the surface of the column also contributed a lot to the performance of the specimen. Furthermore, based on the experimental results, diagonal cracks developed only in the lower block. Therefore, in AEM model, smaller meshes were used only in the lower block (Fig.7), to reduce analysis time with reliable results.

(1) Interface material between concrete blocks and PVC sheet

There must be little bond between the PVC sheet and the concrete blocks, therefore the bearing material explained in section 4 was reasonably adopted for the interface between concrete blocks and PVC sheet

(Fig.7). In order to expect small friction at this interface, the shear modulus (G) and friction coefficient (μ) of the bearing interface were set as reasonably small values.

(2) Interface material between concrete columns and steel plates

In this simulation, elastic material was adopted to model the epoxy resin used between the concrete blocks and the steel plates (Fig.7). The elastic material with Young's modulus of 100N/mm^2 and separation strain of 1.0 were used for the analysis.

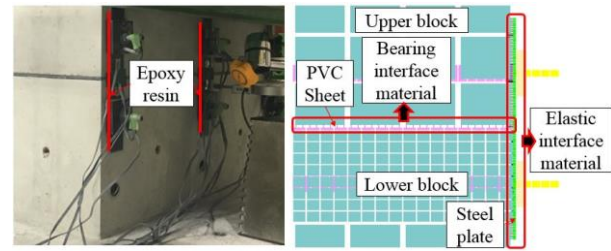


Fig.7 The interface material in model Case 1

(3) Verification of simulation

Fig.8 and Fig.9 illustrate that the bearing interface material with $\mu=0.2$ and $G=5\text{N/mm}^2$ or the bearing interface material with $\mu=0.1$ and $G=30\text{N/mm}^2$ showed reliable results of load-displacement relationship in monotonic analysis and those modeling were successfully verified by cyclic analysis.

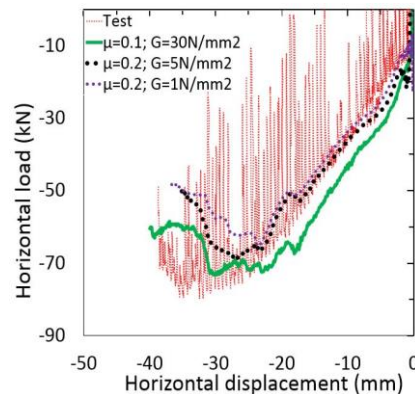


Fig.8 Monotonic analysis

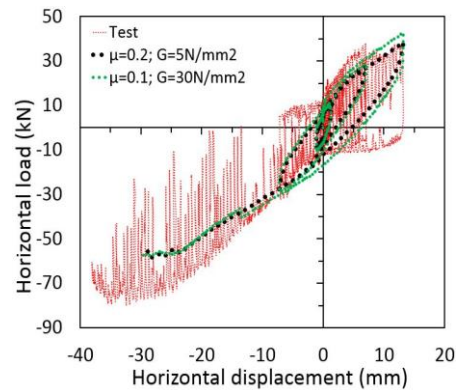


Fig.9 Cyclic analysis

In the cyclic analysis of AEM model, the crack patterns, the failure mode showed good agreement with the experimental results (Fig.10). In details, the diagonal cracks were observed in the

lower block. The failure of the steel bar occurred in the simulation when horizontal displacement was -30mm while that in the test happened at -35mm at the same location.

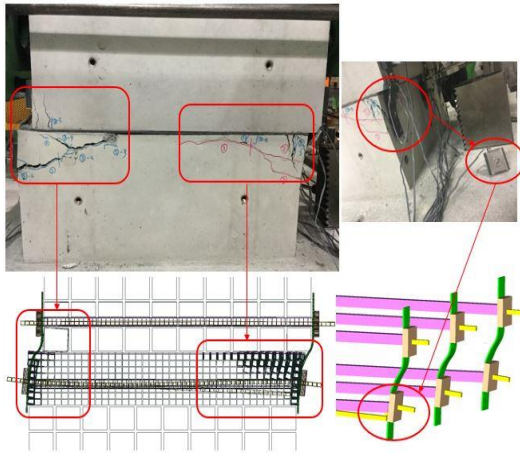


Fig.10 Cracks and failure patterns

5.2 Case 2

In the experiment, spongy pads of 60x60x3mm were inserted between the steel plates and the surface of the column creating small gap of 3mm (Fig.11). Then, it was observed that the contact between the steel plates and surface of the column just occurred after 5mm horizontal displacement was applied.

The load was almost constant until the displacement was increased up to around 5mm, because the load bearing mechanism was mainly governed by the friction between the PVC sheet and the concrete blocks (Fig.5).

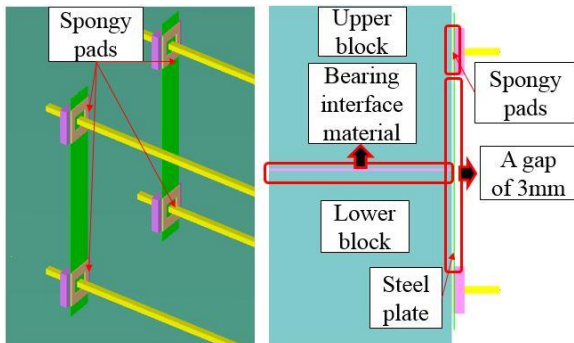


Fig.11 The interface material in model Case 2

(1) Interface material between concrete blocks and PVC sheet

The PVC sheets used in Case 2 and Case 1 were almost the same in terms of mechanical properties and the thickness. The modeling of the bearing interface material between the concrete column and the PVC can be verified also in Case 2.

(2) Verification of simulation

The simulation results demonstrated that only bearing interface material with $\mu=0.2$ and $G=5N/mm^2$ showed good agreement with experimental results in monotonic analysis (Fig.12) and successfully verified by cyclic analysis (Fig.13).

However, due to the unsmooth surface of the PVC sheet, the upper block showed rocking. The

sliding and rocking behavior of the upper block caused unequal compression to the lower block and hence spalling of concrete in one side of it. In AEM, where the PVC sheet was assumed to have a smooth surface, this unexpected spalling, was not observed. In addition, the failure of steel plates in AEM model of Case 2 was observed at different positions compared to the positions in the test (Fig.14).

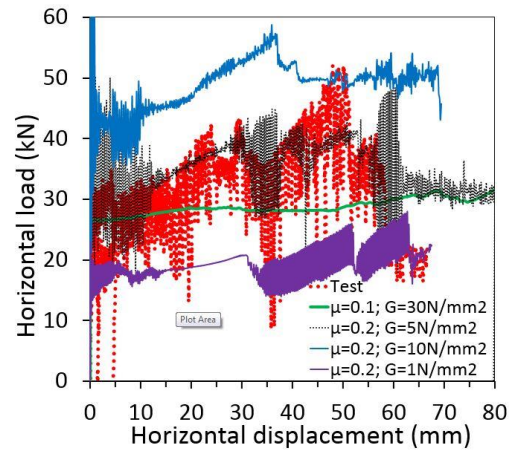


Fig.12 Monotonic analysis

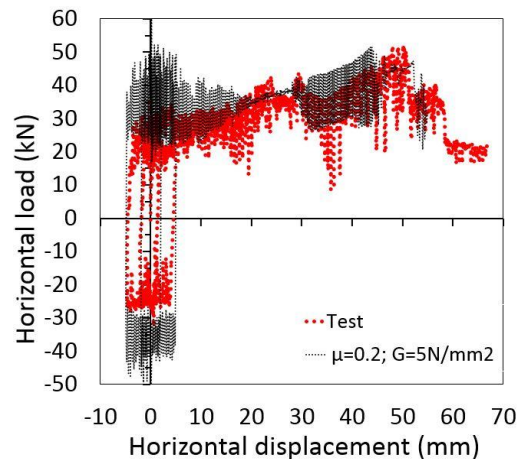


Fig.13 Cyclic analysis

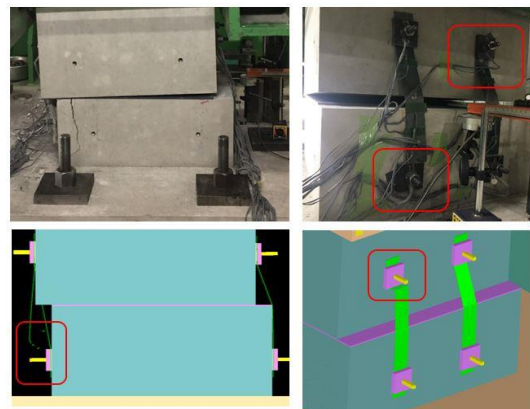


Fig.14 Cracks and failure patterns

5.3 Case 3

(1) Interface material between concrete blocks and PVC sheet

Since the PVC sheet was changed to a soft-thin sheet, the interface material between concrete blocks

and the PVC sheet was appropriately redefined.

(2) Verification of simulation

Fig.15 and Fig.16 illustrates that the bearing interface material with $\mu=0.1$ and $G=0.1\text{N/mm}^2$ showed good agreement in monotonic analysis and successfully verified by cyclic analysis. After some sliding of the upper block, the specimen started cracking at the joint between lower concrete block and footing. The rocking behavior in AEM simulation was obtained at almost corresponding time with the test when 27mm of horizontal displacement was applied to the specimen. No failure was found in the grid-steel plate retrofitting system. Fig. 17 shows the comparable rocking behavior of the specimen in AEM simulation and in the test.

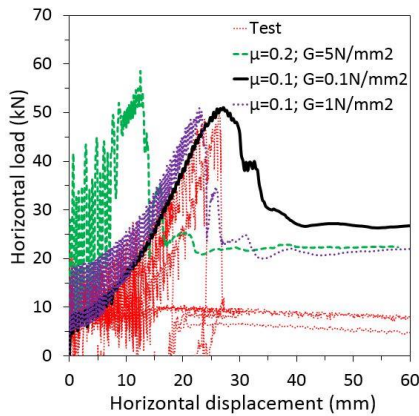


Fig.15 Monotonic analysis

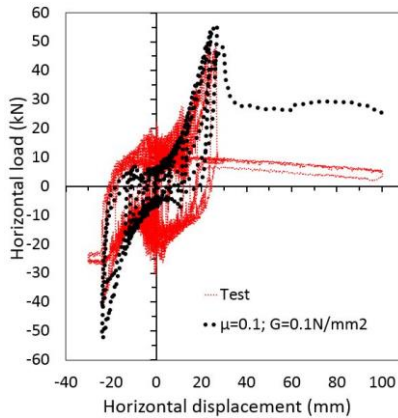


Fig.16 Cyclic analysis

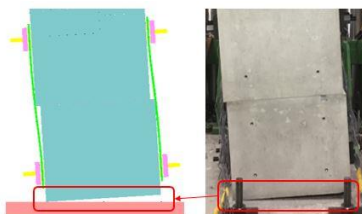


Fig.17 The rocking behavior of the column

6. CONCLUSIONS

Based on the experimental results and numerical simulations using AEM, the following conclusions are drawn from this research.

(1) The grid-steel plate retrofitting method showed good contribution to mitigate the sliding behavior

of the retrofitted column at the joint and caused rocking behavior at the base.

- (2) The details of grid-steel plate retrofitting method were important to avoid unexpected local failure such as diagonal cracking of concrete, the rupture of steel bars connecting steel plates. With some improvements based on the lessons from the first two cases, the last case in experiment showed preferable retrofitted performance.
- (3) The experimental results have been successfully simulated by the AEM models in terms of the load-displacement relationship, cracks in the concrete specimen and failure patterns of the grid-steel plate system.
- (4) The modeling for bearing materials used at the interface between the concrete blocks and the PVC sheet was important to obtain reliable simulation results. Appropriate friction coefficient and shear modulus were obtained in this research.

REFERENCES

- [1] “Guideline for repair and retrofit of masonry and plain concrete structures”, Japan National Railways, Structure Design Office, Feb. 1987. (in Japanese).
- [2] Tadokoro, T., Tottori, S., Hattori, H., “Experiment and Finite Element Analysis for Flexural and Shear Behavior of Masonry Piers”, RTRI REPORT, Vol. 19(12), Dec. 2005, pp. 39-44.
- [3] Meguro, K. and Tagel-Din, H. S., “Applied element method used for large displacement structural analysis”, Journal of Natural Disaster Science, Vol. 24(1), 2002, pp. 25-34.
- [4] Meguro, K. and Tagel-Din, H. S., “Applied element method for dynamic large deformation analysis of structures”, Doboku Gakkai Ronbunshu, Vol. 17(661), 2000, pp. 1-10.
- [5] Helmy, H., Salem, H. and Mourad, S., “Computer-aided assessment of progressive collapse of reinforced concrete structures according to GSA code”, Journal of Performance of Constructed Facilities, Vol. 27(5), 2012, pp. 529-539.
- [6] Maekawa, K. and Okamura, H., “The deformational Behavior and Constitutive Equation of Concrete using the Elasto-plastic and Fracture Model”, Journal of the Faculty of Engineering, The University of Tokyo (B), Vol. 37(2), 1983, pp. 253-328.
- [7] Ristic, D., Yamada, Y. and Iemura, H., “Stress-strain based modeling of hysteretic structures under earthquake induced bending and varying axial loads”, Research report, School of Civil Engineering, Kyoto University, No. 86-ST-01, 1986.
- [8] International, A.S.: p. LLC (ASI) www.appliedscienceint.com.
- [9] Salem, H., Mohssen, K., Kosa, K. and Hosoda, A., “Collapse analysis of Utatsu Ohashi bridge damaged by Tohoku tsunami using applied element method”, Journal of Advanced Concrete Technology, Vol. 12(10), 2014, pp. 388-402.